In-Plane Magnetization-Induced Quantum Anomalous Hall Effect

Xin Liu, Hsiu-Chuan Hsu, and Chao-Xing Liu*

Department of Physics, The Pennsylvania State University, University Park, Pennsylvania 16802-6300, USA

(Received 14 March 2013; published 20 August 2013)

The quantum Hall effect can only be induced by an out-of-plane magnetic field for two-dimensional electron gases, and similarly, the quantum anomalous Hall effect has also usually been considered for systems with only out-of-plane magnetization. In the present work, we predict that the quantum anomalous Hall effect can be induced by in-plane magnetization that is not accompanied by any out-of-plane magnetic field. Two realistic two-dimensional systems, Bi_2Te_3 thin film with magnetic doping and HgMnTe quantum wells with shear strains, are presented and the general condition for the in-plane magnetization-induced quantum anomalous Hall effect is discussed based on the symmetry analysis. Nonetheless, an experimental setup is proposed to confirm this effect, the observation of which will pave the way to search for the quantum anomalous Hall effect in a wider range of materials.

DOI: 10.1103/PhysRevLett.111.086802 PACS numbers: 73.43.−f, 72.25.Dc, 75.50.Pp, 85.75.−d

Introduction.—For a two-dimensional (2D) electron gas in an out-of-plane magnetic field, a transverse voltage can be driven by the Lorentz force felt by electrons, known as the Hall effect, which was first discovered by E. H. Hall in 1879 [1]. Later, Hall also observed the stronger transverse voltage in ferromagnetic conductors with an out-of-plane magnetization, dubbed the anomalous Hall effect [2,3], where the Hall effect is induced by the exchange coupling of magnetic ions and spin-orbit coupling in the band structure. The Hall effect has its quantum version, the quantum Hall effect [4], in which the out-of-plane magnetic field is essential to form Laudau levels and obtain the quantized Hall conductance. In recent years, it was realized that the anomalous Hall effect also has its quantum version, dubbed the quantum anomalous Hall (QAH) effect [5–7]. Recently, several realistic systems, including Mn doped HgTe quantum wells [8], magnetic impurities doped Bi_2Se_3 thin films [9], $GdBiTe_3$ thin films [10], etc. [11,12], have been proposed for the QAH effect and a large experimental effort has been made to pursue the realization of this effect in the presence of an out-of-plane magnetization [13–15]. However, the out-of-plane magnetization is usually accompanied by an out-of-plane magnetic field. Topologically, the QAH state can be adiabatically connected to the quantum Hall state, so it is not easy to distinguish them when an out-of-plane magnetic field coexists with the magnetization.

In this Letter we propose to realize the QAH in a 2D system with an in-plane magnetic field to exclude the orbital effect from the out-of-plane magnetic field. The breaking of time reversal (TR) symmetry, which is a necessary condition for the nonzero Hall conductance, occurs for any direction and any type of magnetization. Therefore, there is no constraint to limit the realization of the QAH effect with in-plane magnetization. Indeed, a concrete theoretical model has been constructed for the QAH effect due to the in-plane magnetic field [16]. In the present work, we find that the QAH effect can generally be induced by a purely in-plane magnetization when breaking both TR and all reflection symmetries. We propose two realistic 2D systems to realize the in-plane magnetization-induced QAH effect, which are accessible in the present experimental conditions.

We start from a general symmetry analysis of the necessary conditions for the appearance of the nonzero Hall conductance. First, the Hall conductance must be zero in a TR invariant system, so a magnetic field or magnetization is required. Besides TR symmetry, the 2D point group (PG) symmetry gives an additional constraint for the Hall conductance, as first shown by Fang [17]. The 2D PGs consist of two families, the n-fold rotation symmetry C_n and the n-fold dihedral symmetry D_n [18]. The dihedral group D_n in 2D PGs is generated by the rotation C_n and the reflection M. Here we emphasize that reflection M in 2D PGs always corresponds to the reflection in three-dimensional (3D) PGs with the reflection plane perpendicular to the 2D plane. The reflection in 2D PGs plays the role of inversion in 3D and distinguishes the pseudoscalar (pseudovector) from the scalar (vector). The Hall conductance is zero if the 2D system has any reflection symmetry M. For example, let us consider a system with the reflection symmetry M_x ($x \to -x$, $y \to y$) in the 2D plane, denoted the xy plane. For the Hall response $j_x = \sigma_{xy}E_y$, under M_x the current j_x changes its sign ($j_x \to -j_x$) while the electric field E_y keeps its sign, so the Hall response equation is changed to $j_x = -\sigma_{xy}E_y$. If the system is invariant under M_x, the response equation should also be invariant under M_x, constraining the Hall conductance σ_{xy} to be zero. Similar arguments can be applied to any 2D reflection symmetry. The out-of-plane magnetization is a pseudoscalar in the 2D PGs, breaking any reflection symmetry M. In contrast, the in-plane magnetization, denoted $\boldsymbol{m}$, is a pseudovector, and there is still a surviving reflection symmetry M_m with the reflection plane perpendicular to $\boldsymbol{m}$; thus, the in-plane

magnetization by itself cannot induce a nonzero Hall conductance and it is necessary to introduce other mechanisms to break the remaining reflection symmetry M_m. The symmetry analysis gives us a guidance to search for the nonzero Hall conductance with in-plane magnetization and below we will present two realistic systems in which not only the nonzero Hall conductance but also the quantum anomalous Hall effect can be realized with in-plane magnetization.

Bi_2Te_3 *thin film with magnetic doping.*—Our first example is the Bi_2Te_3 thin film with magnetic doping, which possesses the QAH effect with an out-of-plane magnetization [9]. Here we will show that the QAH effect can also be induced by in-plane magnetization in this system once we take into account the threefold warping term [19]. The low energy physics of a magnetically doped Bi_2Te_3 thin film is dominated by the two surface states on the top and bottom surfaces, with the Hamiltonian given by [9,20]

$$H = \left(\hbar v_F(\hat{\boldsymbol{z}} \times \boldsymbol{k}) \cdot \boldsymbol{\sigma} + \frac{\lambda}{2}(k_+^3 + k_-^3)\sigma_z\right)\tau_z + \boldsymbol{g} \cdot \boldsymbol{\sigma} \quad (1)$$

in the basis $|t\uparrow\rangle$, $|t\downarrow\rangle$, $|b\uparrow\rangle$, and $|b\downarrow\rangle$, where t (b) is for the top (bottom) surface and $\uparrow$ ($\downarrow$) is for spin up (spin down). The Pauli matrices $\boldsymbol{\sigma}$ denote spin operators and $\tau_z = +1(-1)$ represent the surface states on the top (bottom) surface. We take the growth direction of the thin film as $\hat{\boldsymbol{z}}$ and the film plane as the xy plane. The first term is the kinetic term with the Fermi velocity v_f; the second term is the threefold warping term with the parameter λ [19]; and the third term gives the spin splitting characterized by the parameters $\boldsymbol{g} = (g_x, g_y, g_z)$. The Zeeman type of spin splitting can originate from the direct Zeeman coupling between the electron spin and the magnetic fields, or from the exchange coupling between the electron spin and the magnetization of the magnetic ions. The direction of $\boldsymbol{g}$ is along the in-plane magnetization $\boldsymbol{m}$. The hybridization between two surface states [9] is neglected here, which is not essential for our discussion below. The QAH effect has been studied for this model when $\lambda = g_x = g_y = 0$ [9], and here we focus on the case when both the in-plane magnetization and the warping term are nonzero. The warping term breaks the full in-plane rotation symmetry down to the threefold rotation (C_3) symmetry along $\hat{\boldsymbol{z}}$, which coincides with the symmetry of the Bi_2Te_3 lattice in Fig. 1(a).

The Bi_2Te_3 thin films have D_3 PG symmetry with three reflection operations $M_{1,2,3}$, which are related to each other by C_3 rotation, with the reflection planes indicated by three black lines in Fig. 1(a). One can easily check that the warping term in the Hamiltonian (1) preserves the x direction reflection $M_x = i\sigma_x$ ($M_x = M_1$) but breaks y direction reflection $M_y = i\sigma_y$, consistent with the lattice symmetry of Bi_2Te_3 in Fig. 1(a). According to the symmetry analysis, we require that the magnetization breaks both the TR symmetry and $M_{1,2,3}$ in order to obtain a nonzero Hall conductance.

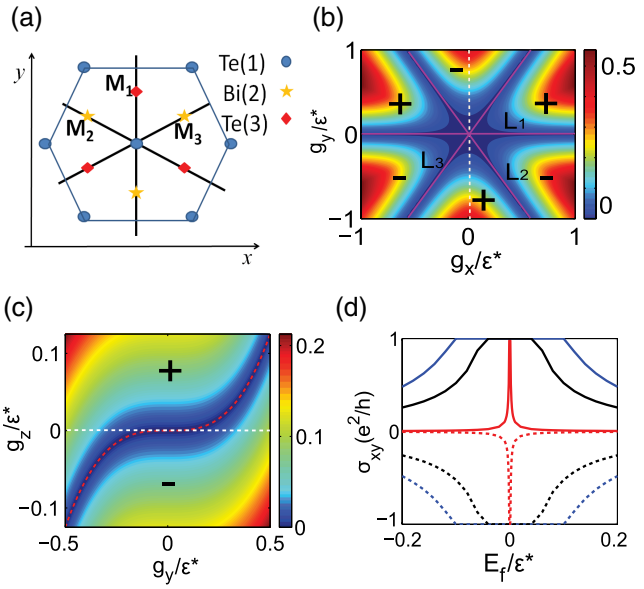

FIG. 1 (color online). In-plane magnetization-induced QAH effect in a Bi_2Te_3 film. (a) Top view of Bi_2Te_3. The blue circles (red rhombuses) represent the Te atoms and the yellow stars represent the Bi atoms. The notation Te(1), Bi(2), Te(3) show the first three atomic layers away from the top surface. The three black lines (M_1, M_2, and M_3) indicate the three reflection planes. (b) The band gap as a function of g_x and g_y. The $g_x - g_y$ plane is divided in six insulating regimes separated by the three metal lines ($L_{1,2,3}$) where the band gap is closed. The $+(-)$ in each area indicates the sign of the Hall conductance. Here the parameters g_x and g_y are rescaled with the energy unit $\varepsilon^* = v/\lambda = 0.23$ eV [19]. (c) The band gap in the $g_y - g_z$ plane. The red solid line indicates the band gap closing. The white dashed line corresponds to the white line in panel (b). (d) The Hall conductance is plotted versus the chemical potential for different magnitudes of the in-plane magnetization. The blue, black, and red solid lines correspond to the y direction magnetization $g_y = -0.5\varepsilon^*$, $-0.3\varepsilon^*$, $-0.1\varepsilon^*$, respectively, while the blue, black, and red dashed lines correspond to $g_y = 0.5\varepsilon^*$, $0.3\varepsilon^*$, $0.1\varepsilon^*$.

Since we are interested in the QAH regime, which requires an insulating state, it is instructive to check the band gap of the Hamiltonian (1), which shows a sixfold pattern as a function of the in-plane magnetization g_x and g_y, as shown in Fig. 1(b). There are six insulating regimes with finite band gaps, which are separated by three gapless lines when the magnetization $\boldsymbol{g}$ is along the direction indicated by the three lines $L_{1,2,3}$ in Fig. 1(b). This result coincides with the early calculation for a single surface [21,22]. Magnetization preserves the reflection symmetry M_i ($i = 1, 2, 3$) when its direction is along the line L_i. Therefore, we expect a zero Hall conductance for the magnetization along the gapless lines $L_{1,2,3}$. For the insulating regimes, the reflection symmetries $M_{1,2,3}$ are broken, so the Hall conductance can be nonzero. To determine the

Hall conductance in the insulating regime, we consider how these insulating regimes are connected to the regimes with a finite out-of-plane magnetization g_z, where the quantized Hall conductance has been determined as in Ref. [9]. Figure 1(c) is plotted for the band gap as a function of g_y and g_z, with the gap closing along the red dashed line. The white dashed line with $g_z = 0$ in Fig. 1(c) corresponds to the white dashed line in Fig. 1(b) with $g_x = 0$. From Fig. 1(c), we find that the insulating regime with positive (negative) g_y and $g_z = 0$ is adiabatically connected to the regimes with negative (positive) g_z and $g_y = 0$. The system with a negative (positive) g_z and $g_y = 0$ should carry a Hall conductance $-(e^2/h)(+(e^2/h))$, as shown in Ref. [9]. Since the quantized Hall conductance cannot vary for two adiabatically connecting insulating regimes, we expect that the Hall conductance is $-(e^2/h)(+(e^2/h))$ for the insulating regime with a positive (negative) g_y and $g_{x,z} = 0$. Due to the C_3 rotation symmetry, we can also determine the Hall conductance in other insulating regimes, as shown by the sign $\pm$ in Fig. 1(b). Moreover, we perform a direct calculation of the Hall conductance based on the Kubo formula [23,24]. As shown in Fig. 1(d), the Hall conductance is quantized when the Fermi energy lies in the band gap, confirming the above analysis. When the Fermi energy is above or below the band gap, the Hall conductance drops down, but is still nonzero. Based on the calculation of the band gap and the Hall conductance, we conclude that the quantized Hall conductance can be induced by the combination of the in-plane magnetization and the threefold warping term in the present model.

The present argument based on the crystal symmetry also provides a way to distinguish the present mechanism from other possible mechanisms for the anomalous Hall conductance, as shown by the experimental setup of the Hall measurement in Fig. 2(a). By rotating the in-plane magnetization, the Hall conductance will switch between $\pm(e^2/h)$ for the insulating regimes, depending on the angle φ between the magnetization and the crystal orientation, as shown in Fig. 2(b). Since there is no out-of-plane magnetic field, the orbital effect can be safely excluded. The recent first principle calculation shows that the in-plane magnetization can open a gap of around 0.25 meV on the surface of topological insulators [21]. Therefore the QAH effect induced by in-plane magnetization is expected below 3 K. For the metallic regimes, as shown by the blue solid and black dashed lines in Fig. 2(b), the Hall conductance is no longer quantized, but still oscillates between positive and negative values with a period φ of $2\pi/3$. This behavior is also different from that of the conventional anomalous Hall effect.

Hg_xMn_{1-x} Te quantum wells with shear strains.—The in-plane magnetization-induced QAH effect is not limited to the concrete example of Bi_2Te_3 thin films, and instead, it can be generalized to other systems by engineering band structures. In the following, we will show how the shear

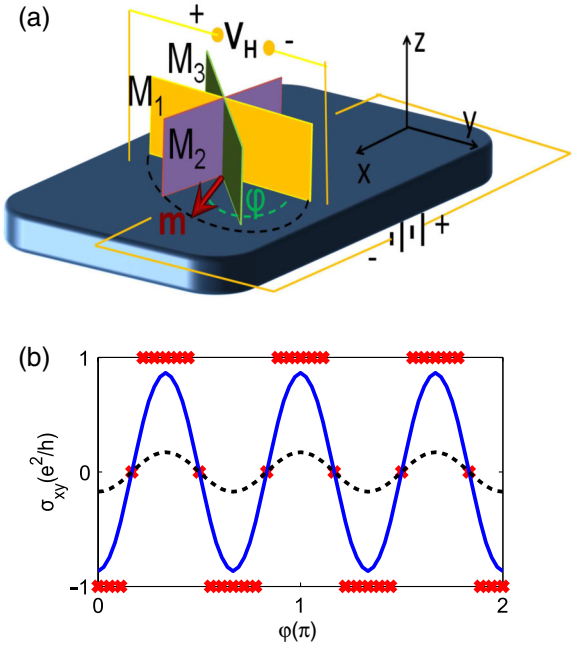

FIG. 2 (color online). Experimental setup. (a) The proposed experimental configuration to confirm the in-plane magnetization-induced QAH effect. The arrow indicates the direction of magnetization. Three planes denote three reflection planes of the Bi_2Te_3 crystal. (b) The Hall conductance is plotted versus the angle of the in-plane magnetization at different Fermi energies. The red crosses, and black dashed and blue solid lines correspond to $E_f = 0$, $-0.002\varepsilon^*$, and $0.02\varepsilon^*$, respectively. The Hall conductance oscillates between $\pm e^2/h$ with a $2\pi/3$ period whether the chemical potential is in the electron or hole band. Here we take $g_y = 0.1\varepsilon^*$ [21].

strain can induce this effect in HgMnTe quantum wells and then discuss the general strategy to search for this effect. The effective model for Mn doped HgTe quantum wells is described by the Bervenig-Hughes-Zhang (BHZ) Hamiltonian with an additional Zeeman type of coupling [25,26]

$$H = H_{\mathrm{BHZ}} + H_g, \tag{2}$$

$$H_{\mathrm{BHZ}} = \varepsilon(\boldsymbol{k}) + \mathcal{M}(\boldsymbol{k})\tau_z + A(k_x\tau_x\sigma_z - k_y\tau_y), \tag{3}$$

$$H_g = \boldsymbol{g}_1 \cdot \boldsymbol{\sigma} + \boldsymbol{g}_2 \cdot \boldsymbol{\sigma}\tau_z \tag{4}$$

in the basis $|E1+\rangle$, $|H1+\rangle$, $|E1-\rangle$, $|H1-\rangle$. Here the Pauli matrices $\boldsymbol{\sigma}$ are for spin and $\boldsymbol{\tau}$ are for the subbands of $E1$ and $H1$. The functions $\varepsilon(\boldsymbol{k})$, $\mathcal{M}(\boldsymbol{k})$, as well as the parameter A, are defined in Ref. [25]. The vectors $\boldsymbol{g}_1 = (1/2)(\boldsymbol{g}_e + \boldsymbol{g}_h)$ and $\boldsymbol{g}_2 = (1/2)(\boldsymbol{g}_e - \boldsymbol{g}_h)$ with $\boldsymbol{g}_{e(h)} = (g_{e(h)x}, g_{e(h)y}, g_{e(h)z})$, which are treated as parameters in the following, describe the spin splitting for the $E1$ ($H1$) subband, and have the same direction as the in-plane magnetization $\boldsymbol{m}$. The BHZ Hamiltonian with the magnetization along the z direction ($g_{1(2)z} \neq 0$) has been studied

in Ref. [27], and the QAH phase is found when g_{2z} is large enough. The BHZ Hamiltonian has the D_∞ symmetry, so any plane perpendicular to the xy plane can serve as the reflection plane. The in-plane magnetization $\boldsymbol{m}$ preserves the reflection symmetry M_m, so the Hall conductance is zero for the BHZ model with in-plane magnetization.

To obtain a nonzero Hall conductance, we need to break the remaining reflection symmetry, which can be achieved by introducing a new term due to the shear strains ϵ_{xz} and ϵ_{yz}, written as

$$H_{\mathrm{str}} = F[\epsilon_{xz}(k_x\sigma_x + k_y\sigma_y) + \epsilon_{yz}(k_x\sigma_y - k_y\sigma_x)]\tau_x \qquad (5)$$

with the parameter F. This form of the Hamiltonian can be derived from the six-band Kane model [26,28], as described in detail in the Supplemental Material [29]. Experimentally, the shear strain appears in the HgTe-HgCdTe superlattices grown on a CdZnTe substrate along an asymmetric direction, such as the (112) direction [30–32]. The ϵ_{xz} (ϵ_{yz}) term breaks the x direction reflection $M_x = i\sigma_x$ (the y direction reflection $M_y = i\sigma_y\tau_z$) and preserves M_y (M_x). Figure 3(a) shows the band gap for the Hamiltonian $H_{\mathrm{BHZ}} + H_m + H_{\mathrm{str}}$ as a function of ϵ_{xz} and g_{2z} with a finite in-plane magnetization g_{1x}. When $\epsilon_{xz} = 0$, the Hall conductance is $+(e^2/h)(-(e^2/h))$ for positive (negative) g_{2z}, as obtained in Ref. [27]. The system is metallic for $g_{2z} = 0$, separating the two QAH phases with opposite Hall conductances. With a finite ϵ_{xz}, we find the gapless line derives away from the line of $g_{2z} = 0$ and the regime with positive (negative) ϵ_{xz} and $g_{2z} = 0$ is adiabatically connected to the regime with positive (negative) g_{2z}, which indicates that the Hall conductance for a positive (negative) ϵ_{xz} is $+(e^2/h)(-(e^2/h))$, as shown in Fig. 3(a). In Fig. 3(b), the band gap is plotted as a function of ϵ_{xz} and ϵ_{yz} with a finite g_{1x}, and a gapless line along $\epsilon_{xz} = 0$ separates two QAH phases with the Hall conductance $\pm(e^2/h)$. The Hall conductance vanishes along the gapless line, because both the shear strain ϵ_{yz} and the in-plane magentization $g_{1(2)x}$ preserve the reflection M_y. More generally, the Hall conductance is always zero when two vectors, the shear strain $\boldsymbol{\epsilon} = (\epsilon_{xz}, \epsilon_{yz})$ and the in-plane magnetization $\boldsymbol{m}$, are perpendicular to each other. We emphasize that the shear strain ϵ_{ij} is a tensor in 3D PGs, but we can treat $\boldsymbol{\epsilon}$ as a vector in 2D PGs. According to Fig. 3(b), we can consider the experimental configuration for the magnetization and shear strain for the HgMnTe quantum wells, similar to that of Bi_2Te_3 thin films, as shown in Fig. 3(c). When the angle φ between the strain vector $\boldsymbol{\epsilon}$ and the magnetization vector $\boldsymbol{m}$ is rotated across $\pi/2$ or $3\pi/2$, the Hall conductance switches between $\pm(e^2/h)$ of the two insulating phases. In Fig. 3(d), we verify the stability of the QAH phases for different values of $\boldsymbol{g}_1$ and the QAH phase always exists when the in-plane magnetization is large enough.

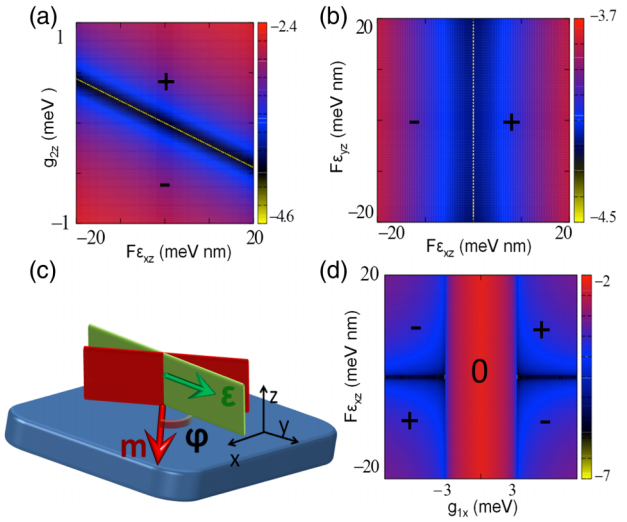

FIG. 3 (color online). In-plane magnetization induced QAH effect in HgMnTe quantum wells. (a) The band gap as a function of g_{2z} and ϵ_{xz} with a finite $g_{1x} = 8$ meV. (b) The band gap as a function of ϵ_{xz} and ϵ_{yz} with $g_{1x} = 4$ meV, $g_{2x} = 3$ meV. (c) Schematic plot of the experimental setup. The angle between the strain vector $\boldsymbol{\epsilon}$ (green arrow) and the magnetization vector $\boldsymbol{m}$ (red arrow) is denoted as φ. The green plane denotes the reflection plane preserved by the strain vector $\boldsymbol{\epsilon}$ while the red plane denotes the reflection plane preserved by the magnetization vector $\boldsymbol{m}$. (d) The band gap as a function of g_{1x} and ϵ_{xz} with $g_{2z} = 0$. The other parameters are taken as $M = -3$ meV, $B = 0.85$ eV $\cdot$ nm^2, $D = 0.67$ eV $\cdot$ nm^2, $A = 0.38$ eV $\cdot$ nm, $g_{1(2)y} = g_{1z} = 0$, and $\epsilon_{yz} = 0$.

Discussion and conclusion.—From the above two examples, we find that the breaking of reflection symmetry is essential for the in-plane magnetization-induced QAH effect. Generally, a pseudoscalar, such as the out-of-plane magnetization, can break all the reflection symmetries in 2D PGs. Therefore, one should also construct a pseudoscalar with the in-plane magnetization. For example, a pseudoscalar, the dot product of a vector and a pseudovector $\boldsymbol{\epsilon} \cdot \boldsymbol{m}$, can be defined to characterize the Hall conductance in the HgMnTe quantum wells with shear strains. As shown in Fig. 3(d), the sign of the Hall conductance is determined by the sign of the product of ϵ_{xz} and g_{1x}. We expect that this strategy can also be applied to search for the QAH phase in other systems.

We propose experiments with rotating in-plane magnetic fields, as shown in Figs. 2(a) and 3(c), to confirm the predicted effect. Since no out-of-plane magnetization is required, the orbital effect from Landau levels of magnetic fields can be excluded completely. Therefore, the proposed setups can provide a clear experimental signal to distinguish the orbital effect of magnetic fields from the exchange effect of magnetic ions. Our proposal is also feasible in experiments since Cr or Mn doped Bi_2Te_3 films or Mn doped HgTe quantum wells have already been realized [13–15]. Moreover, ferromagnetic materials are usually metallic, preventing the appearance of the QAH effect which requires insulating materials. The existing

ferromagnetic insulators, such as EuO and GdN, have in-plane magnetization for a thin film configuration [33–35]. Therefore, the in-plane magnetization-induced QAH effect will pave the way to the new QAH materials with hybrid structures made of ferromagnetic insulators.

We would like to thank Jainendra Jain, Laurens Molenkamp, Xiao-Liang Qi, Nitin Samarth, Yayu Wang, Qikun Xue, and Shoucheng Zhang for useful discussions. X. L. acknowledges partial support by the U.S. DOE under Award No. DE-SC0005042.

*cxl56@psu.edu

[1] E. H. Hall, Am. J. Math. **2**, 287 (1879).
[2] E. H. Hall, Philos. Mag. **12**, 157 (1881).
[3] N. Nagaosa, J. Sinova, S. Onoda, A. H. MacDonald, and N. P. Ong, Rev. Mod. Phys. **82**, 1539 (2010).
[4] K. v. Klitzing, G. Dorda, and M. Pepper, Phys. Rev. Lett. **45**, 494 (1980).
[5] F. D. M. Haldane, Phys. Rev. Lett. **61**, 2015 (1988).
[6] M. Onoda and N. Nagaosa, Phys. Rev. Lett. **90**, 206601 (2003).
[7] X. L. Qi, Y. S. Wu, and S. C. Zhang, Phys. Rev. B **74**, 045125 (2006).
[8] C.-X. Liu, X.-L. Qi, X. Dai, Z. Fang, and S.-C. Zhang, Phys. Rev. Lett. **101**, 146802 (2008).
[9] R. Yu, W. Zhang, H.-J. Zhang, S.-C. Zhang, X. Dai, and Z. Fang, Science **329**, 61 (2010).
[10] H.-J. Zhang, X. Zhang, and S.-C. Zhang, arXiv:1108.4857.
[11] C. Wu, Phys. Rev. Lett. **101**, 186807 (2008).
[12] Z. Qiao, S. A. Yang, W. Feng, W.-K. Tse, J. Ding, Y. Yao, J. Wang, and Q. Niu, Phys. Rev. B **82**, 161414 (2010).
[13] C.-Z. Chang, J.-S. Zhang, M.-H. Liu, Z.-C. Zhang, X. Feng, K. Li, L.-L. Wang, X. Chen, X. Dai, Z. Fang, X.-L. Qi, S.-C. Zhang, Y. Wang, K. He, X.-C. Ma, and Q.-K. Xue, Adv. Mater. **25**, 1065 (2013).
[14] D. Zhang, A. Richardella, S. Xu, D. W. Rench, A. Kandala, T. C. Flanagan, H. Beidenkopf, A. L. Yeats, B. B. Buckley, P. V. Klimov, D. D. Awschalom, A. Yazdani, P. Schiffer, M. Z. Hasan, and N. Samarth, Phys. Rev. B **86**, 205127 (2012).
[15] H. Buhmann, J. Liu, Y. S. Gui, V. Daumer, M. Koenig, C. R. Becker, and L. W. Molenkamp, in *Physics of Semiconductors—2002*, Proceedings of the 15th International Conference on High Magnetic Fields in Semiconductor Physics, Oxford, 2002, edited by A. R. Long and J. H. Davies, IOP Conf. Proc. No. 171 (Institute of Physics, Bristol, 2003).
[16] Y. Zhang and C. Zhang, Phys. Rev. B **84**, 085123 (2011).
[17] C. Fang, M. J. Gilbert, and B. A. Bernevig, Phys. Rev. B **86**, 115112 (2012).
[18] M. S. Dresselhaus, G. Dresselhaus, and A. Jorio, *Group Theory: Application to the Physics of Condensed Matter* (Springer, New York, 2008).
[19] L. Fu, Phys. Rev. Lett. **103**, 266801 (2009).
[20] C.-X. Liu, X.-L. Qi, H. J. Zhang, X. Dai, Z. Fang, and S.-C. Zhang, Phys. Rev. B **82**, 045122 (2010).
[21] J. Henk, M. Flieger, I. V. Maznichenko, I. Mertig, A. Ernst, S. V. Eremeev, and E. V. Chulkov, Phys. Rev. Lett. **109**, 076801 (2012).
[22] L. Oroszlány and A. Cortijo, Phys. Rev. B **86**, 195427 (2012).
[23] D. J. Thouless, M. Kohmoto, M. P. Nightingale, and M. den Nijs, Phys. Rev. Lett. **49**, 405 (1982).
[24] N. A. Sinitsyn, J. E. Hill, H. Min, J. Sinova, and A. H. MacDonald, Phys. Rev. Lett. **97**, 106804 (2006).
[25] B. A. Bernevig, T. L. Hughes, and S. C. Zhang, Science **314**, 1757 (2006).
[26] W. Beugeling, C. X. Liu, E. G. Novik, L. W. Molenkamp, and C. Morais Smith, Phys. Rev. B **85**, 195304 (2012).
[27] C.-X. Liu, X.-L. Qi, X. Dai, Z. Fang, and S.-C. Zhang, Phys. Rev. Lett. **101**, 146802 (2008).
[28] E. G. Novik, A. Pfeuffer-Jeschke, T. Jungwirth, V. Latussek, C. R. Becker, G. Landwehr, H. Buhmann, and L. W. Molenkamp, Phys. Rev. B **72**, 035321 (2005).
[29] See Supplemental Material at http://link.aps.org/supplemental/10.1103/PhysRevLett.111.086802 for the derivation of effective Hamiltonian for HgMnTe quantum wells with shear strain.
[30] M. Li, C. R. Becker, R. Gall, W. Faschinger, and G. Landwehr, Appl. Phys. Lett. **71**, 1822 (1997).
[31] S. Hatch, R. Sewell, J. Dell, L. Faraone, C. Becker, and B. Usher, J. Electron. Mater. **35**, 1481 (2006).
[32] M. Li, R. Gall, C. R. Becker, T. Gerhard, W. Faschinger, and G. Landwehr, J. Appl. Phys. **82**, 4860 (1997).
[33] T. Kasuya and D. X. Li, J. Magn. Magn. Mater. **167**, L1 (1997).
[34] P. G. Steeneken, L. H. Tjeng, I. Elfimov, G. A. Sawatzky, G. Ghiringhelli, N. B. Brookes, and D.-J. Huang, Phys. Rev. Lett. **88**, 047201 (2002).
[35] T. S. Santos, J. S. Moodera, K. V. Raman, E. Negusse, J. Holroyd, J. Dvorak, M. Liberati, Y. U. Idzerda, and E. Arenholz, Phys. Rev. Lett. **101**, 147201 (2008).